 

PACS numbers: 42.70.Dm; 64.70.Md
DOI: 10.1070/QE2004v034n12ABEH002743

# Reversible orientation first-order transitions induced in a nematic liquid crystal by a spatially limited light beam and a low-frequency electric field

A.S. Zolot'ko, M.P. Smayev, V.F. Kitaeva, M.I. Barnik

***Abstract*. A new type of reversible orientation first-order transitions in a nematic liquid crystal (NLC) in the optical and low-frequency electric fields is studied experimentally and theoretically. It is shown that these transitions, characterised by a distinct bistability of the director field both upon variation of the light beam power $P$ (the low-frequency electric-field voltage $U = \text{const}$) and the electric-field voltage $U$ ($P = \text{const}$), are related to a finite diameter of the light beam and the oblique incidence of the beam on the NLC.**

***Keywords***: *liquid crystals, light-induced reorientation, phase transitions, optical bistability*.

## 1. Introduction

The molecular structure of nematic liquid crystals (NLCs) is extremely sensitive to external perturbations. Thus, the action of weak low-frequency fields [1, 2] and the electric field of a light wave induces the Fredericksz transitions.

The experimental and theoretical studies performed upon normal incidence of a light wave on NLCs showed that the reverse influence of the crystal on the light field could transform the orientation second-order Fredericksz transitions in crossed light and low-frequency fields [3, 4] to the first-order transitions [5 – 15]*. In this case, an increase or decrease in the power of an extraordinary polarised light beam (in homotropic NLCs) or low-frequency voltage (in planar NLCs) provided a reversible switching between two stable states [9 – 12, 14, 15]; this switching occurs jumpwise and is characterised by the hysteresis (bistability) of the director field.

A finite diameter of the light beam is not important in these effects. The width of bistability regions is determined by the material parameters of the NLC and is rather small (for example, the relative width of the bistability region in [10 – 12] was less than 0.02 upon variation of the light beam power and 0.05 upon variation of the low-frequency voltage).

A light beam of a finite diameter incident obliquely on a crystal can also induce reversible first-order transitions of another type (we will call them 'geometrical' transitions). Let us explain qualitatively this mechanism by the example of a planar oriented NLC with the positive dielectric anisotropy. In such a crystal, the two degenerate states $\boldsymbol{n}_1(\boldsymbol{r})$ and $\boldsymbol{n}_2(\boldsymbol{r})$ of the director field can be induced by the above-threshold low-frequency field. These states differ only in the sense of the director rotation from the unperturbed state $\boldsymbol{n}_0$ and, therefore, they are mirror symmetric with respect to the NLC walls. The director-field state in a real crystal depends on a small pretilt on the crystal walls; let it be the state $\boldsymbol{n}_1(\boldsymbol{r})$. If the angle between the light field $\boldsymbol{E}$ and $\boldsymbol{n}_2(\boldsymbol{r})$ is smaller than the angle between $\boldsymbol{E}$ and $\boldsymbol{n}_1(\boldsymbol{r})$ (which is possible in the case of oblique incidence of light on the crystal), the light-induced transition from the $\boldsymbol{n}_1(\boldsymbol{r})$ state to the $\boldsymbol{n}_2(\boldsymbol{r})$ state can occur in the central part of the beam. After the removal (or decrease) of the field $\boldsymbol{E}$, the reverse switching occurs due to elastic forces caused by the transverse spatial inhomogeneity of the director (on the light-beam periphery, i.e., where $\boldsymbol{E} = 0$, the orientation of the director field $\boldsymbol{n}_1(\boldsymbol{r})$ is preserved). The observation of the described reversible transition, which proved to be the first-order transition accompanied by a distinct hysteresis, was briefly reported in [16]. The reversible first-order transition can also occur in this case upon variation of the low-frequency field voltage [16, 17]*.

However, the orientation transitions observed upon the interaction of NLCs with a light beam of a finite size and a low-frequency field were not theoretically analysed so far.

The aim of this paper is to study first of all theoretically the 'geometrical' orientation transitions and also to investigate experimentally the orientation hysteresis in more detail and compare the theory with experiment.

## 2. Experimental

We studied a ZhKM-1282 crystal doped with a KD-1 diazodye (weight content 0.025 %) whose planar orientation

* In the case of propagation of an extraordinary light wave in an NLC, no change in the transition order was observed in the absence of an additional low-frequency field (although it can occur theoretically [13]). In the case of elliptic (in particular, circular) polarisation of light, the transition order changes in the absence of a low-frequency field as well [6 – 8].

* The switching between the two stable states of the director field was also realised in homotropically oriented NLCs by rotating them with respect to the direction of the magnetic [18] and electric [19] fields.

**A.S. Zolot'ko, M.P. Smayev, V.F. Kitaeva** P.N. Lebedev Physics Institute, Russian Academy of Sciences, Leninskii prosp. 53, 119991 Moscow, Russia; e-mail: zolotko@sci.lebedev.ru;
**M.I. Barnik** A.V. Shubnikov Institute of Crystallography, Russian Academy of Sciences, Leninskii prosp. 59, 117333 Moscow, Russia; e-mail: lcl@ns.crys.rus.ru

Received 20 April 2004; revision received 30 September 2004
*Kvantovaya Elektronika* **34** (12) 1151 – 1156 (2004)
Translated by M.N. Sapozhnikov

was achieved by rubbing a polymer (polyimide) coating of substrates. The nematic ZhKM-1228 matrix is a mixture of biphenyls and esters and has a positive low-frequency dielectric anisotropy $\Delta\varepsilon_{\mathrm{low\,f}} = 9.9$ ($\nu = 1$ kHz, $t = 20\,^{\circ}$C). The threshold voltage $U_{\mathrm{th}}$ of the Fredericksz transition in a planar oriented crystal is 1.1 V. The refractive indices of ZhKM-1228 are $n_{\parallel} = \varepsilon_{\parallel}^{1/2} = 1.68$ and $n_{\perp} = \varepsilon_{\perp}^{1/2} = 1.51$ ($\lambda = 589$ nm).

We doped the NLC with a KD-1 dye because in this case a light beam produces the torque $\boldsymbol{\Gamma}_{\mathrm{opt}}$, which exceeds by more than an order of magnitude the torque produced in the pure NLC (the director $\boldsymbol{n}$ in planar crystals is oriented in this case parallel to the light field $\boldsymbol{E}$) [20, 21]. The sample thickness was $L \simeq 100$ μm.

The structural formula of the KD-1 dye has the form

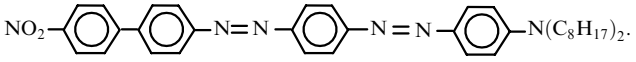


A 532-nm light beam from a solid-state laser was focused into a crystal by a lens with the focal distance $f = 18$ cm (the waist diameter was about 100 μm). The polarisation plane of the light beam was rotated with the help of a double Fresnel rhomb. The plane of a liquid-crystal layer was vertical, and the unperturbed director $\boldsymbol{n}_0$ was located in the horizontal plane. The angle of incidence $\alpha$ of light on the crystal can be varied by rotating a cell with the NLC around the vertical axis. It was equal to 52° in the described experiment. The light beam diameter was varied by moving the cell with respect to the focal plane of the lens to the diverging part of the beam. A low-frequency (3 kHz) electric field was applied to $SnO_2$ electrodes deposited on the inner walls of the flat cell with the NLC.

The light-induced reorientation of the director was accompanied by the light beam self-action, resulting in the appearance of aberration rings [21, 22], whose number characterises the rotation angle of the director.

We studied the dependence of the number $N$ of aberration rings on the light beam power $P$, which was continuously increased or decreased (the low-frequency voltage $U$ was constant), as well as the dependence of $N$ on $U$, which was continuously increased and decreased ($P =$ const). On passing to each new value of power or voltage, the number $N$ was measured after $\sim 5$ min, when the rings were stabilised.

## 3. Experimental results

### 3.1 Orientation transition and bistability of the director field upon changing the light beam power ($U =$ const)

Studies were performed at four voltages $U = 1.1$, 1.2, 1.35, and 1.45 V. A crystal was located in the focal plane of the lens or was displaced from it by the distance $\Delta = 16$ cm. Figure 1 shows the results obtained.

For low powers $P \leqslant 1$ mW, the aberration pattern was not observed. As the beam power was increased, the aberration pattern appeared and the number of rings increased. For some power $P_{\mathrm{high}}$, typical for a given (rather high) voltage and the distance $\Delta$ from the focal plane (Figs 1a, c–e), the number of rings drastically increased ($N \simeq 25 - 30$). As the beam power was further increased, the number of rings was not changed substantially. The number of rings decreased with decreasing the beam power. For some beam power $P_{\mathrm{low}}$, the aberration pattern collapsed abruptly, and only one spot was observed on the screen ($P_{\mathrm{low}} < P_{\mathrm{high}}$).

One can see from Figs 1a, e that for $U = 1.45$ V, the displacement of the cell from the focal plane to the diverging beam by the distance $\Delta = 16$ cm leads to the increase in the bistability region from 1 to 8 mW.

The increase of the voltage from 1.2 to 1.45 V applied to the cell displaced by 16 cm from the focal plane leads to the increase in the bistability region from 1 to 8 mW (Figs 1c–e). Bistability disappeared with decreasing voltage applied to the crystal (Fig. 1b).

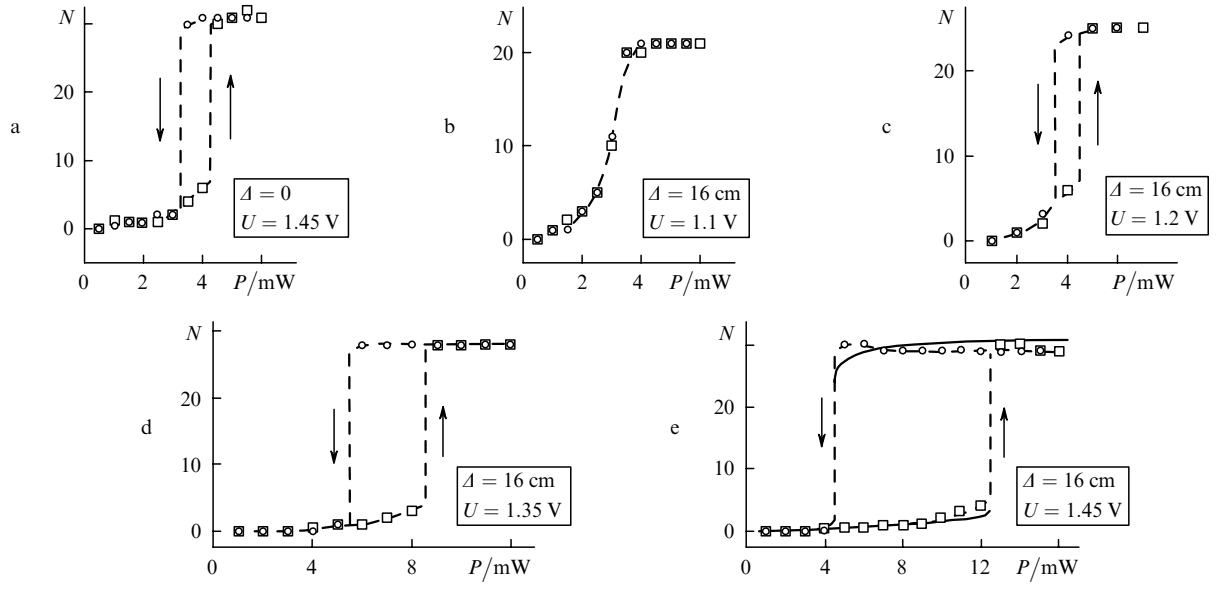


**Figure 1.** Experimental (□, ○) and theoretical (e, solid curves) dependences of the number $N$ of aberration self-focusing rings in a light beam transmitted through a planar NLC (thickness $L = 100$ μm, $\lambda = 532$ nm, angle of incidence $\alpha = 52°$) obtained by increasing (□) and decreasing (○) the beam power $P$ for different displacements $\Delta$ of the NLC from the focal plane and an applied low-frequency (3 kHz) voltage $U$.

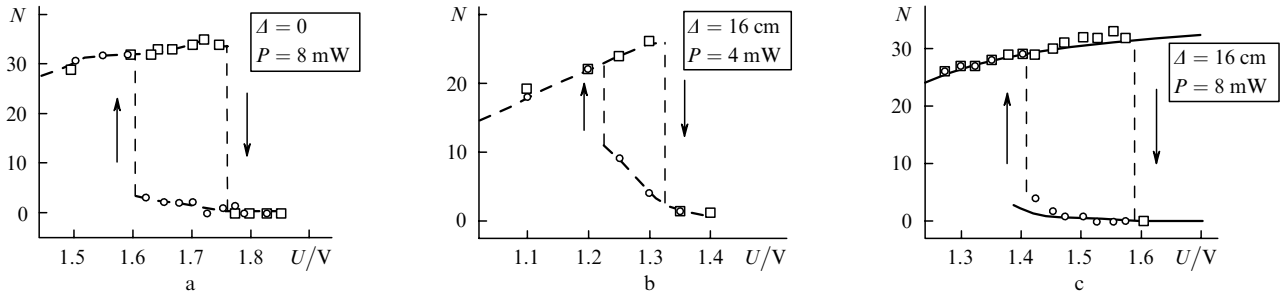


**Figure 2.** Experimental (□, ○) and theoretical (c, solid curves) dependences of the number $N$ of aberration self-focusing rings in a light beam transmitted through a planar NLC (thickness $L = 100\mu$m, $\lambda = 532$ nm, angle of incidence $\alpha = 52^\circ$) obtained by increasing (□) and decreasing (○) the low-frequency (3 kHz) voltage $U$ for different displacements $\Delta$ of the NLC from the focal plane and the light-beam power $P$.

### 3.2 Orientation transition and the director field bistability upon changing the voltage $U$ ($P$ = const)

Studies were performed for $\Delta = 0$ and 16 cm and $P = 4$ and 8 mW. Figure 2 presents the results obtained.

It follows from Fig. 2 that the increase in the voltage $U$ first leads to the increase in the number $N$ of self-focusing rings. The maximum number of the rings observed was $N_{\max} = 32$. At some voltage $U_{\text{high}}$, the aberration pattern collapsed during 2–3 min and only one bright spot was observed on the screen. As the voltage was further increased, the aberration pattern did not change.

As the voltage $U$ was decreased, the rings appeared again and their number $N$ slowly increased. At some voltage $U_{\text{low}}$, the number of rings abruptly increased to the value that was already observed at this voltage, and the dependence $N(U)$ which was observed earlier was repeated with decreasing voltage.

One can see from Figs 2a, c that the displacement of the crystal from the focal plane to the diverging beam weakly expands the bistability region.

The width of the bistability region for the crystal displaced by 16 cm from the focal plane increased with increasing the light beam power. Thus, the increase of $P$ from 4 to 8 mW resulted in the increase in the width of the bistability region from 0.1 to 0.17 V (Figs 2b, c).

Therefore, the experimental study of the orientation first-order phase transitions show that the width of the bistability region depends on the light-beam diameter and power, as well as on the low-frequency voltage of the electric field. The relative widths of bistability regions observed in this paper exceed by an order of magnitude the widths obtained in [10–12].

## 4. Theoretical analysis and comparison with experiments

Let us analyse now theoretically the 'geometrical' reversible orientation first-order transition.

We will derive the equation for the time dependence $\boldsymbol{n}(\boldsymbol{r}, t)$ of the director field by writing the equilibrium condition for the torques acting on the director:

$$\boldsymbol{\Gamma}_{\text{visc}} + \boldsymbol{\Gamma}_{\text{elast}} + \boldsymbol{\Gamma}_{\text{elect}} + \boldsymbol{\Gamma}_{\text{opt}} = 0, \tag{1}$$

where $\boldsymbol{\Gamma}_{\text{visc}} = \gamma_1[\boldsymbol{n} \times \mathrm{d}\boldsymbol{n}/\mathrm{d}t]$ is the viscous torque; $\gamma_1$ is the viscosity coefficient; $\boldsymbol{\Gamma}_{\text{elast}} = K[\boldsymbol{n} \times \Delta\boldsymbol{n}]$ is the elastic torque in the single-constant approximation; $K$ is the Frank elastic constant; $\boldsymbol{\Gamma}_{\text{elect}} = (\Delta\varepsilon_{\text{low f}}/4\pi)\ (\boldsymbol{nV})[\boldsymbol{n} \times \boldsymbol{V}]$ in the torque due to the external quasi-stationary electric field $\boldsymbol{V}$; $\boldsymbol{V} = \boldsymbol{e}_y U \sin 2\pi\nu t$; $\boldsymbol{e}_y$ is the unit vector along the $Y$ axis perpendicular to the crystal walls (Fig. 3); and

$$\boldsymbol{\Gamma}_{\text{opt}} = \frac{\Delta\varepsilon_{\text{eff}}}{4\pi}\ (\boldsymbol{nE})[\boldsymbol{n} \times \boldsymbol{E}] \tag{2}$$

is the torque associated with intermolecular forces appearing due to absorption of light by dye molecules [23]. Here,

$$\boldsymbol{E} = \frac{1}{2}\,\boldsymbol{e}A \exp[-\mathrm{i}(\boldsymbol{kr} - \omega t)] + \text{c.c.}; \tag{3}$$

$A$ is the complex amplitude of the light wave entering the NLC; $\boldsymbol{e} = \boldsymbol{e}_x \cos\beta - \boldsymbol{e}_y \sin\beta$ is the unit polarisation vector of the extraordinary wave; $\boldsymbol{e}_x$ is the unit vector along the $X$ axis;

$$\Delta\varepsilon_{\text{eff}} = \Delta\varepsilon f_0\left[\cos^2\ (\psi + \beta) - \sin^2\beta_{\text{c}}\right] \tag{4}$$

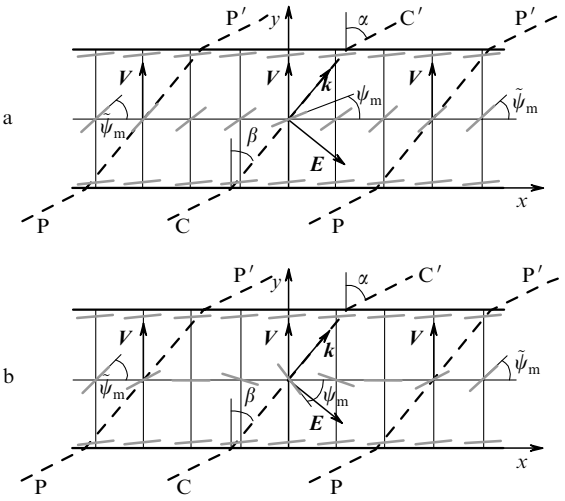


**Figure 3.** Two stable configurations of the director field of a planar NCL in a light beam and low-frequency electric field $\boldsymbol{V}$: (a) the director field configuration with the positive angle $\psi_{\text{m}}$ of its maximum rotation on the CC′ axis of the light beam (corresponds to branches AB in Fig. 4a and DE in Fig. 5b); and (b) the director field configuration with the negative angle $\psi_{\text{m}}$ (corresponds to branches CD in Fig. 4a and AC in Fig. 5b); $\boldsymbol{k}$ and $\boldsymbol{E}$ are the wave vector and electric field of the light beam; $\tilde{\psi}_{\text{m}}$ is the rotation angle of the director in the periphery (PP′) of the light beam. The short grey straight lines show the director orientation $\boldsymbol{n}$ at different points of the NLC; $\alpha$ and $\beta$ are the angles of incidence and refraction of the light beam, respectively.

is the effective optical anisotropy [17, 23]; $\Delta\varepsilon = \varepsilon_{\parallel} - \varepsilon_{\perp}$ is the ordinary optical anisotropy; $f_0 \sim 10^2$ is the material parameter of the NLC characterising the efficiency of the orienting action of light on the crystal director; and $\beta_c = 15^\circ$ is the critical angle [20, 21]. We neglected in (2) a direct orienting action of the light field on the induced dipoles because it is much weaker than the action caused by the dye.

By substituting the components

$$n_x = \sin\psi, \quad n_y = \cos\psi, \quad n_z = 0 \tag{5}$$

of the director field into (1) and performing averaging over the time $\sim 1/v$ [which is much shorter than the characteristic reorientation time of the director ($\sim 10$ s)], we obtain the equation

$$\frac{\partial\psi}{\partial t} = K\left(\frac{\partial^2\psi}{\partial x^2} + \frac{\partial^2\psi}{\partial y^2} + \frac{\partial^2\psi}{\partial z^2}\right) + \frac{\Delta\varepsilon_{\mathrm{low\,f}} V_0^2}{8\pi}\sin\psi\cos\psi + \frac{\Delta\varepsilon_{\mathrm{eff}}|A|^2}{8\pi}\sin(\psi+\beta)\cos(\psi+\beta). \tag{6}$$

The solution of partial differential equation (6) for the function $\psi(x, y, z, t)$ is a complex problem. Because we are interested first of all in the orientation of the director on the light-beam axis, we replace the transverse Laplacian $(\partial^2/\partial x^2 + \partial^2/\partial z^2)\psi$ by the expression $(\psi - \tilde{\psi})/b^2$, where $\psi(y, t)$ now denotes the director field on the beam axis, $\tilde{\psi}(y, t)$ is the director field on the beam periphery, and $b$ is a parameter of the order of the beam radius. In this approximation, restricting ourselves to the first spatial harmonics of the functions $\psi(y, t)$ and $\tilde{\psi}(y, t)$ [$\psi(y, t) = \psi_m(t)\sin(\pi y/L)$, $\tilde{\psi}(y, t) = \tilde{\psi}_m(t)\sin(\pi y/L)$], we reduce equation (6) to the form

$$\dot{\psi}_m = -\psi_m + \delta_{el} J_1(2\psi_m) - \eta\tilde{H} - g(\psi_m - \tilde{\psi}_m), \tag{7}$$

where $\tilde{H} = \frac{1}{2}F - F\sin^2\beta_c + \frac{1}{4}H$; $F = J_1(2\psi_m)\cos 2\beta E_1(2\psi_m) \times \sin 2\beta$; $H = J_1(4\psi_m)\cos 4\beta + E_1(4\psi_m)\sin 4\beta$; $\delta_{el} = U^2/U_{th}^2$ is the square of the normalised low-frequency voltage applied to the NLC; $U_{th} = (\pi/L)(8\pi K\Delta\varepsilon_{\mathrm{low\,f}}^{-1})^{1/2}$ is the threshold voltage of the Fredericksz transition in the low-frequency field; $\eta = pf_0/p_{th}$ is the dimensionless power density of the light wave on the light-beam axis; $p = cn_e|A|^2/8\pi$; $p_{th} = (\pi^2/L^2)(cn_eK/\Delta\varepsilon)$ is the threshold power density of the light-induced Fredericksz transition in the homeotropically oriented NLC; $g = L^2/(\pi^2 b^2)$; and $J_1(x)$ and $E_1(x)$ are the first-order Bessel and Weber functions. The power of a Gaussian beam with the waist $w$ is $P = \pi w^2 p/2$, so that the parameter $\eta$ can be represented in the form $\eta = P/P_0$, where $P_0 = P_{th}/f_0$ and $P_{th} = \pi w^2 p_{th}/2$. The function $\tilde{\psi}_m$ is determined by the equation

$$-\tilde{\psi}_m + \delta_{el} J_1(2\tilde{\psi}_m) = 0, \tag{8}$$

which is obtained from (7) for $\eta = 0$. It is obvious that $g = 0$ for a plane light wave.

The dependences of the stationary solutions of Eqn. (7) for $\psi_m$ on the parameters $\eta$ and $\delta_{el}$ are presented in Figs 4 and 5. The dependences $\psi_m(\eta)$ in Figs 4a, c were calculated using the experimental value $\delta_{el} = 1.74$ ($U = 1.45$ eV) and different values of the parameter $g$ characterising the beam diameter. The values of $g$ (Figs 4a–c) and $P_0 = 3.07$ mW (Fig. 4a) were fitted to the experimental dependences presented in Figs 1a, e. One can see from Fig. 4a that the dependence $\psi_m(\eta)$ consists of the two stable (AB and CD) and one unstable (CB) branches. The branches AB and CB correspond to the positive angles $\psi_m$, while the branch CD corresponds to the negative angles $\psi_m$. The corresponding stable configurations of the director field are shown schematically in Fig. 3.

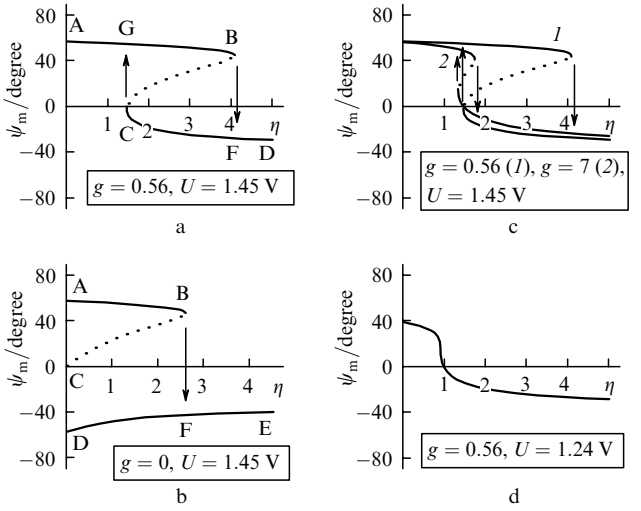


**Figure 4.** Theoretical dependences of the rotation angle $\psi_m$ of the director on the dimensional power density $\eta$ of the light wave on the light beam axis for an obliquely incident light beam of a finite diameter (a, c, d) and a plane light wave (b). Stable and unstable states are shown by solid and dotted curves, respectively.

Let us discuss this in more detail. In the absence of the light field $\boldsymbol{E}$ ($\eta = 0$, point A), the director $\boldsymbol{n}$ turns under the action of the low-frequency field $\boldsymbol{V}$. The sense of this rotation is determined by the pretilt of the director on the crystal walls. The rotation will be counter-clockwise with respect to the unperturbed orientation of the director ($\psi_m \approx 0$) in the case of the pretilt shown in Fig. 3a. When the crystal was illuminated by a light beam of a finite diameter and the beam power (parameter $\eta$) was increased, the angle $\psi_m$ decreased (the director rotated clockwise, i.e., tended to orientate parallel to the light field) and abruptly passed, at some value of $\eta$ corresponding to the point B, to the negative branch of $\psi_m$ (point F on the CD branch), i.e., to another stable configuration (Fig. 3b).

The jumpwise nature of the transition means that the torques $\boldsymbol{\Gamma}_{elast}$, $\boldsymbol{\Gamma}_{elect}$, and $\boldsymbol{\Gamma}_{opt}$ cannot be in equilibrium within a certain interval $\psi_F < \psi_m < \psi_B$. For example, for $\psi_m = 0$, the torque $\boldsymbol{\Gamma}_{elect}$ is obviously zero, and therefore the orienting action of the light wave (torque $\boldsymbol{\Gamma}_{opt}$) cannot be compensated in the case of a rather broad beam by the elastic torques $\boldsymbol{\Gamma}_{elast}$ caused by the transverse inhomogeneity of the director.

Let us assume now that the light beam power (parameter $\eta$) is decreased. Because of the transverse inhomogeneity, the director field configuration becomes unstable.* At some value of $\eta$ corresponding to the point C, abrupt transition occurs to the point C on the AB branch (i.e., the return to the configuration of the director field shown in Fig. 3a).

* The instability of such a configuration of the director field in the absence of the light field was observed in [24].

Let us compare the results of theoretical calculations and experimental measurements of the number $N$ of aberration rings (i.e., in fact, of the rotation angle of the director). The passage from the theoretical dependence $\psi_m(\eta)$ to the dependence $N(P)$ is performed with the help of the relation

$$N = \frac{N_0}{\cos\beta}\{[J_0(2\psi_m) - J_0(2\tilde{\psi}_m)]\cos 2\beta + [E_0(2\psi_m) - E_0(2\tilde{\psi}_m)]\sin 2\beta\} \quad (9)$$

(where $N_0 = \delta n L/2\lambda$ and $\delta n = \varepsilon_{\|}^{1/2}\Delta\varepsilon/2\varepsilon_{\perp}$), which is derived in Appendix.

One can see from Fig. 1e that the calculated dependence of the number $N$ of aberration rings on $P$ is very close to the experimental dependence.

The theoretical dependence $\psi_m(\eta)$ for a plane light wave ($g = 0$) presented in Fig. 4b shows that the angle $\psi_m$ changes with increasing $\eta$ as in the case of a beam of a finite diameter. However, unlike the latter case, as $\eta$ is decreased, no reverse transition from negative to positive angles $\psi_m$ occurs (from the DE to AB branch), which is explained by the absence of the transverse inhomogeneity of the director field.

Because the direct transition (with increasing $\eta$) occurs irrespective of the light beam width, while the reverse transition (with decreasing $\eta$) occurs only when the beam diameter is restricted, these transitions should obviously take place at different values of the power density $\eta$, which explains the presence of the hysteresis (Fig. 4a).

Figure 4c shows the dependence of the width of the bistability region on the light-beam diameter. One can see that the bistability region narrows down with decreasing the beam diameter and is displaced to lower powers. Such a behaviour corresponds to the experimental data (Figs 1a, e).

The dependence of the width of the bistability region on the voltage $U$ also agrees with the experiment. Our calculations show that the width of the bistability region decreases with decreasing $U$, and bistability disappears completely for $U = 1.24$ V ($\delta_{el} = 1.27$) (Fig. 4d). This is also observed experimentally; however, bistability disappears when $U$ lies in the interval $1.1\text{ V} < U < 1.2\text{ V}$ (Figs 1b, c), which is somewhat lower than the theoretical value.

Let us describe now theoretically the orientation transitions and bistability observed upon variation of a low-frequency field. Figure 5 shows the dependences $\psi_m(\delta_{el})$ for a plane wave and a light beam of a finite diameter calculated by (7). For $U = 0$, the director turns clockwise under the action of the light field ($\psi_m < 0$, point A). In the case of a plane light wave, the electric field only increases the absolute value of this angle (Fig. 5a, the AB branch), while the transition to the positive values of $\psi_m$ (the DC branch) is absent. In the case of a light beam of a finite diameter (Fig. 5b), this transition (from the point C of the AC branch to the point F of the DE branch) occurs*.

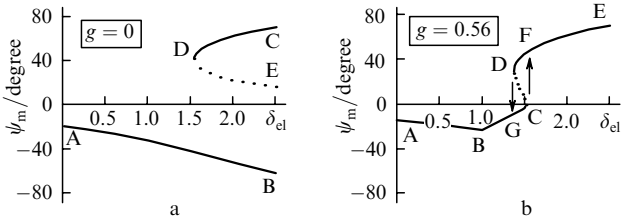


**Figure 5.** Theoretical dependences of the rotation angle $\psi_m$ of the director on the parameter $\delta_{el}$ for an obliquely incident plane light wave (a) and a light beam of a finite diameter (b) for $P = 4$ mW. Stable and unstable states are shown by solid and dotted curves, respectively.

The theoretical dependence of the width $\Delta U$ of the bistability region on $P$ agrees in general with the experimental dependence. The width increases with $P$, as in the experiment, however, its value differs from the experimental one: for $P = 4$ mW, we have $\Delta U_{theor} < \Delta U_{exp}$ ($\Delta U_{theor} = 0.06$ V, $\Delta U_{exp} = 0.1$ V), for $P = 8$ mW, the width $\Delta U_{theor} > \Delta U_{exp}$ ($\Delta U_{theor} = 0.6$ V, $\Delta U_{exp} = 0.18$ V).

The discrepancy between the theory and experiment can be explained by the fact that the longitudinal dependence of the rotation angle of the director was approximated in the theory only by one lowest harmonic (which is especially manifested for large values of $U$). As for the theoretical dependence $N(U)$, it follows from Fig. 2c that this dependence correctly describes not only the corresponding experimental dependence but also the number of aberration rings.

The theoretical dependence of $U_{low}$ on $\Delta$ also agrees with the experiment: in both cases, $U_{low}$ decreases with increasing $\Delta$. In this case, the theoretical and experimental values of $U_{low}$ are close (1.55 and 1.61 V for $\Delta = 0$, and 1.40 and 1.41 V for $\Delta = 16$ cm).

We calculated bistability for the NLC doped with the KD-1 dye whose interaction with light is characterised by the effective optical anisotropy $\Delta\varepsilon_{eff}$ [17]. A specific feature of $\Delta\varepsilon_{eff}$ for this crystal is its dependence (4) on the mutual orientation of the director and light field. The natural question arises: What will be observed when $\Delta\varepsilon_{eff} = \text{const}$ (i.e., for example, in the case of transparent NLCs, when the ordinary dielectric anisotropy $\Delta\varepsilon = \text{const}$ is used instead of $\Delta\varepsilon_{eff}$). Our calculation of the dependence of the rotation angle of the director on the dimensionless power density $\eta_{tr} = \eta/f_0$ of the light beam for a transparent ZhKM-1282 crystal with the help of the equation

$$\dot{\psi}_m = -\psi_m + \delta_{el}J_1(2\psi_m) + \eta f_0 F - g(\psi_m - \tilde{\psi}_m), \quad (10)$$

which replaces (7) in this case, showed (Fig. 6) that the bistability of the director field also should be observed in a transparent NLC (in accordance with the qualitative picture of the effect presented above). However, it reveals itself at substantially higher powers of the light beam because $\Delta\varepsilon \ll \Delta\varepsilon_{eff}$ in the experimental geometry.

## 5. Conclusions

We have studied a new type of reversible orientation first-order transitions in a NLC illuminated by an obliquely incident light beam of a finite diameter in a low-frequency electric field.

* Note that the solution, which is similar to that presented in Fig. 5a, was obtained in [24], where the transition between the states with the angles $\psi_m$ of opposite signs was observed with increasing the low-frequency field voltage. However, the properties of this transition were not studied experimentally.

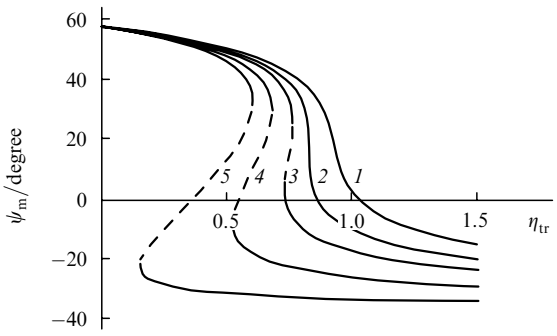


**Figure 6.** Theoretical dependences of the rotation angle $\psi_m$ of the director on the dimensionless power density $\eta_{tr}$ of the light wave on the axis of a light beam of a finite diameter obliquely incident on a transparent NLC in a low-frequency electric field ($\delta_{el} = 1.74$); $g = 0.56$ (*1*), 0.47 (*2*), 0.4 (*3*), 0.3 (*4*), and 0.2 (*5*).

These transitions were observed both upon variation of the light-beam power $P$ (at low-frequency voltage $U =$ const) and upon variation of $U$ ($P =$ const). We have found that the widths of the corresponding bistability regions increased with increasing voltage $U$, power $P$, and the light-beam diameter. The obtained widths of bistability regions exceed approximately by an order of magnitude the values typical of the orientation reversible transitions observed at the normal incidence of a light wave.

We have developed a simple theoretical model of orientation transitions, which explains the basic experimental results. It is shown that the reversible switching between different states of the director field upon 'geometrical' transitions is caused by the mutual orientation of the light and low-frequency fields, as well as by a finite diameter of the light beam.

***Acknowledgements.*** The authors thank V.N. Ochkin for useful discussions. This work was supported by the Russian Foundation for Basic Research (Grant Nos 02-02-16927 and 04-02-17354) and the Federal Programs 'Integration' (Grant B0049) and 'Studies and Development in the Priority Areas of the Science and Technology'.

## Appendix

The number of aberration rings formed in the cross section of a light beam transmitted through a NLC is [22]

$$N = \frac{\Delta S_{nl}}{2\pi}, \tag{A1}$$

where

$$\Delta S_{nl} = \frac{2\pi}{\lambda \cos\beta} \int_0^L \left[ n_e^a(y) - n_e^p(y) \right] dy \tag{A2}$$

is the nonlinear phase shift on the beam axis; $n_e^a$ and $n_e^p$ are the refractive indices of the extraordinary light wave on the beam axis and its periphery, respectively.

We use the known expression for the refractive index of the extraordinary wave

$$n_e = \frac{(\varepsilon_\perp \varepsilon_\parallel)^{1/2}}{\left(\varepsilon_\perp \sin^2\psi' + \varepsilon_\parallel \cos^2\psi'\right)^{1/2}}, \tag{A3}$$

where $\psi'$ is the angle between the wave vector and director. On the beam axis, we have

$$\psi'^{(a)} = \psi_m \sin\frac{\pi y}{L} \tag{A4}$$

and in its periphery,

$$\psi'^{(p)} = \tilde{\psi}_m \sin\frac{\pi y}{L}. \tag{A5}$$

By substituting (A2)–(A5) into (A1), we obtain (9).

## References

1. de Gennes P.G. *The Physics of Liquid Crystals* (Oxford: Clarendon Press, 1975; Moscow: Mir, 1977).
2. Blinov L.M. *Elektro- i magnitooptika zhidkikh kristallov* (Electro- and Magnetooptics of Liquid Crystals) (Moscow: Nauka, 1978).
3. Pikin S.A. *Strukturnye prevrashcheniya v zhidkikh kristallakh* (Structural Transformations in Liquid Crystals) (Moscow: Nauka, 1981).
4. Zolot'ko A.S., Kitaeva V.F., Kuyumchan V.A., Sobolev N.N., Sukhorukov A.P. *Pis'ma Zh. Eksp. Teor. Fiz.*, **36**, 66 (1982) [*JETP Lett.*, **36**, 80 (1982)].
5. Arakelyan S.M. *Usp. Fiz. Nauk*, **153**, 679 (1987).
6. Santamato E., Daino B., Romagnoli M., Settembre M., Shen Y.R. *Phys. Rev. Lett.*, **57**, 2423 (1986).
7. Zolot'ko A.S., Sukhorukov A.P. *Pis'ma Zh. Eksp. Teor. Fiz.*, **52**, 707 (1990) [*JETP Lett.*, **52**, 62 (1990)].
8. Vella A., Piccirillo B., Santamato E. *Phys. Rev. E*, **65**, 031706 (2002).
9. Karn A.J., Arakelian S.M., Shen Y.R., Ong H.L. *Phys. Rev. Lett.*, **57**, 448 (1986).
10. Chen Shu-Hsia, Wu J.J. *Appl. Phys. Lett.*, **52**, 1998 (1988).
11. Wu J.J., Ong Gan-Sing, Chen Shu-Hsia. *Appl. Phys. Lett.*, **53**, 1999 (1988).
12. Wu J.J., Chen Shu-Hsia. *J. Appl. Phys.*, **66**, 1065 (1989).
13. Ong Hiap Liew. *Phys. Rev. A*, **28**, 2393 (1983).
14. Ong Hiap Liew. *Phys. Rev. A*, **31**, 3450 (1985).
15. Ong Hiap Liew. *Phys. Rev. A*, **33**, 3550 (1986).
16. Zolot'ko A.S., Smayev M.P., Kitaeva V.F., Barnik M.I. *Kratk. Soobshch. Fiz. FIAN*, (3), 7 (2004).
17. Barnik M.I., Kharchenko S.A., Kitaeva V.F., Zolot'ko A.S. *Mol. Cryst. Liq. Cryst.*, **375**, 363 (2002).
18. Karn A.J., Shen Y.R., Santamato E. *Phys. Rev. A*, **41**, 4510 (1990).
19. Terskov D.B., Zolot'ko A.S., Barnik M.I., Rumyantsev V.G. *Mol. Materials*, **6**, 151 (1996).
20. Barnik M.I., Zolot'ko A.S., Rumyantsev V.G., Terskov D.B. *Krisallogragiya*, **40**, 746 (1995) [*Crystallogr. Rep.*, **40**, 691 (1999)].
21. Kitaeva V.F., Zolot'ko A.S., Barnik M.I. *Mol. Materials*, **12**, 271 (2000).
22. Zolot'ko A.S., Kitaeva V.F., Sobolev N.N., Sukhorukov A.P. *Zh. Eksp. Teor. Fiz.*, **81**, 933 (1981) [*Sov. Phys. JETP*, **54**, 496 (1981)].
23. Zolot'ko A.S. *Pis'ma Zh. Eksp. Teor. Fiz.*, **68**, 410 (1998) [*JETP Lett.*, **68**, 437 (1998)].
24. Janossy I., Prasad S.K. *Phys. Rev. E*, **63**, 041795 (2001).